
HYPERBOLIC EMBEDDING OF BRAIN NETWORKS DETECTS REGIONS DISRUPTED BY NEURODEGENERATION

Alice Longhena

Paris Brain Institute, CNRS-UMR7225, Inserm-U1127, Sorbonne University-UM75, Inria-Paris.
Pitié Salpêtrière University Hospital. Paris, France
alice.longhena@icm-institute.org

Martin Guillemaud Fabrizio De Vico Fallani

Paris Brain Institute, CNRS-UMR7225, Inserm-U1127, Sorbonne University-UM75, Inria-Paris.
Pitié Salpêtrière University Hospital. Paris, France

Raffaella Lara Migliaccio

Paris Brain Institute, CNRS-UMR7225, Inserm-U1127, Sorbonne University-UM75, Inria-Paris.
Pitié Salpêtrière University Hospital. Paris, France
Institut de Neurologie, Pitié Salpêtrière University Hospital, AP-HP Paris, France

Mario Chavez

CNRS UMR 7225
Hôpital de la Pitié Salpêtrière. Paris, France

July 24, 2024

ABSTRACT

Graph theoretical methods have proven valuable for investigating alterations in both anatomical and functional brain connectivity networks during Alzheimer's disease (AD). Recent studies suggest that representing brain networks in a suitable geometric space can better capture their connectivity structure. This study introduces a novel approach to characterize brain connectivity changes using low-dimensional, informative representations of networks in a latent geometric space. Specifically, the networks are embedded in the Poincaré disk model of hyperbolic geometry. Here, we define a local measure of distortion of the geometric neighborhood of a node following a perturbation. The method is applied to a brain networks dataset of patients with AD and healthy participants, derived from DWI and fMRI scans. We show that, compared with standard graph measures, our method identifies more accurately the brain regions most affected by neurodegeneration. Notably, the abnormality detection in memory-related and frontal areas are robust across multiple brain parcellation scales. Finally, our findings suggest that the geometric perturbation score could serve as a potential biomarker for characterizing disease progression.

Keywords Brain Networks · Geometric embedding · Alzheimer's disease

1 Introduction

Network analysis of brain connectivity has advanced our understanding of the organizational mechanisms underlying different brain states. Interestingly, graph analysis of brain networks has also led to the development of biomarkers that quantify reorganization mechanisms in brain diseases [1, 2]. In particular neurodegenerative diseases like Alzheimer's disease have garnered significant attention from the network neuroscience community [3, 4].

Classic late-onset Alzheimer's disease (AD) is a neurodegenerative disorder that causes progressive cognitive and functional impairments. It is histopathologically characterized by the appearance of amyloid- β plaques [5] and tau-related neurofibrillary tangles, which lead to neuronal loss, brain atrophy, and disrupted normal inter-neuronal connectivity. This leads to a gradual breakdown of cerebral tissue and disrupts both anatomical and functional communication between affected brain regions. The loss of long-range white matter bundles has been shown to impact anatomical brain connectivity in several areas, particularly the parietal and temporal lobes. At the whole connectivity level, these disruptions are evident from an increased characteristic path length and decreased communication efficiency (as compared to healthy subjects) of brain networks estimated from diffusion tensor imaging (DTI) [6, 7]. Similar connectivity alterations have also been documented in resting-state brain networks estimated from functional magnetic resonance imaging (fMRI) [8, 9, 10], as well as from magnetoencephalographic (MEG) [11] and electroencephalographic (EEG) signals [12].

According to the anatomopathological model proposed by Braak and Braak [13], the pathology typically spreads from the medial temporal areas, in particular from the entorhinal cortex, to the hippocampal formation. At later stages, it eventually progresses into the isocortex, from posterior to anterior regions. Clinically, this spreading pattern corresponds to the initial appearance of episodic memory disturbances, followed by deficits in temporal-spatial orientation, language difficulties, praxic planning issues, and problems with object and face recognition. In later stages, disorders of the "frontal" sphere appear, leading to executive impairments and behavioral changes such as increased apathy, agitation, and inappropriate social behavior. Consistent with histopathological and neuropathological models, network-based studies have detected connectivity changes in the temporal lobe, particularly in the hippocampus [14, 15], in early AD stages, which reflect the memory-related symptoms. Other studies report topological changes in the frontal regions [6], associated with behavioral deficits. However, not always the abnormality of an AD biomarker (a certain measurable indicator of the state of the disease) correlate with clinical symptoms severity [16]. Some biomarkers become abnormal before the associated symptoms appear, and they can be crucial for the diagnosis (diagnostic biomarkers) or progression tracking (progression biomarkers) of the disease.

In recent years, network models have shown great potential for embedding brain connectivity graphs into latent spaces where nodes are represented as low-dimensional vectors [17, 18] or probabilistic density functions [19, 18]. Network embeddings are made so that some properties of the original graph structure, usually measures of similarity and proximity between nodes, are maximally preserved in these spaces [20, 18]. By representing networks as vectors or functions, a wide variety of machine learning algorithms can be used to provide a solution for network visualization, link prediction, node classification and node clustering [18]. Most of the current studies embed brain networks into Euclidean spaces to study its connectivity properties [21, 22]. However, such embeddings often require the use of high dimensions and fail to encompass some graph topological properties typical of complex real-world networks, such as hierarchical structure and high clustering [23, 24]. In the case of tree-like structures, as the number of nodes grows exponentially with their distance from the nodes of higher hierarchy, the dimension required to correctly represent these nodes in Euclidean space considerably increases. Nevertheless, increasing the dimensionality leads to increased computational complexity and high distortion of the representation [23, 25]. In contrast, non-Euclidean (hyperbolic) mapping methods require a reduced dimension to accurately embed graphs and better capture their scale-free and hierarchical structure [24].

Hyperbolic embedding has recently been found to encode, with minimal distortion and low computational cost, both local and global topological information of the original graphs [19]. The interest of the scientific community has thus shifted towards finding latent hyperbolic space models capable of explaining the emergence of complex network structures. Indeed, it has been demonstrated that heterogeneous degree distribution and high clustering emerge naturally from the metric definition of spaces with negative curvature [26]. When applied to anatomical brain networks from healthy subjects, hyperbolic embedding has revealed a multiscale connectivity structure between the anatomical brain regions [27]. In a recent work, this geometric representation has shed new lights on the characterization and localization of network perturbations produced by brain surgery in epilepsy [28]. Similarly, a recent study on functional brain networks estimated from MEG signals has shown that hyperbolic embedding can be a useful tool to explore brain network perturbations associated with cognitive decline in Alzheimer's disease [29].

Here, we investigate the advantage of a geometric measure based on hyperbolic representations of brain (anatomical and functional) networks in identifying regions disrupted by neurodegeneration. Our approach involves the use of hyperbolic coalescent mapping to embed a graph in the Poincaré disk [30], a two-dimensional model of hyperbolic geometry. Given the embeddings, we estimate the geometric score recently developed in [28] for each node in brain networks of patients diagnosed with the disease, with respect to healthy controls. This metric has shown a good localization power and a small bias to characterize and localize connectivity perturbations related to edges removal [28]. In the present study, we test its ability to localize the most significant regional perturbations, following connectivity disruption, due to the progression of the disease. Finally, we assessed the role of the spatial scales (the number of nodes used to estimate the networks) on the identification of disrupted regions.

2 Methods

2.1 Data

The dataset used for this study comprises 23 patients diagnosed with Alzheimer’s disease, and 25 healthy participants. For each one of them, we dispose of a functional brain network, derived from functional magnetic resonance imaging (fMRI), and a structural brain network, derived from diffusion-weighted magnetic resonance imaging (DWI), representing the functional and structural connectivity at the moment the scans were performed. Demographic information and neurological characterisation of the participants are reported in Table 1. Additionally, 92% of them report being right-handed. We display the results of the Mini Mental Status Exam (MMSE), a 30-point questionnaire to measure cognitive impairment; the results of free and cued selective reminding test[31, 32] for episodic memory. Specifically, this includes Total Recall (Free+Cued) (TR (F+C)) of 48 items, delayed (20 minutes) Free (FR) and Cued (CR) Recall of 16 items, False Recognitions and Intrusion errors of items. All subjects gave written informed consent for participation in the study, which was approved by the local ethics committee of the Pitié Salpêtrière Hospital in Paris. All experiments were conducted in accordance with relevant guidelines and regulations.

Female/Male	AD (n = 23)			HC (n = 25)			
	12/11	Median	Range	NA	Median	Range	NA
Age (years)	74	[55,87]		69	[34,88]		
Education (years)	9	[5,22]		14	[5,20]		
MMSE (/30)	23	[15,29]		29	[25,30]	1	
TR (F+C)	34	[22,47]	2	47	[43,48]	1	
CR (delayed) (/16)	4	[0,11]	2	12	[7,16]	1	
False Recognition	0.5	[0,8]	1	0	[0,1]	1	
Intrusions	2	[0,15]	2	0	[0,4]	1	

Table 1: Demographic and neurological characterization of subjects. Data is given as Median and Range. Unavailable data are reported as NA. AD: Alzheimer’s disease; HC: healthy controls. MMSE: Mini Mental Status Exam; TR (F+C): Total Recall (Free+Cued); CR: Cued Recall.

The structural brain networks were derived from connectivity matrices based on DWI images, as detailed in [33]. These matrices’ elements estimate connection strength (the number of fiber tracts) between N anatomical regions of interest (network nodes) defined by the Lausanne2008 brain atlas [34, 35]. In functional brain networks, links represent statistically significant correlations between the BOLD fMRI time-series of atlas-defined brain areas. This study focused on wavelet correlation matrices representing functional connectivity in the frequency range 0.05-0.10 Hz [36]. Notably, both fMRI and DWI networks are referenced to the same atlas, enabling region-specific comparison between the two modalities. Further details on dataset acquisition and pre-processing (DTI and fMRI) are available in [33]. We constructed networks considering brain atlas parcellations at different scales: $N = 82$, $N = 128$, and $N = 233$ regions of interest (ROIs), corresponding to the number of nodes.

Connectivity matrices are initially associated to fully connected weighted graphs. To optimize the information of brain networks, we first applied a threshold proportional filtering, retaining a proportion $0 < p < 1$ of the strongest links. As demonstrated in [37], the value of links density that optimizes the trade-off between efficiency (both local and global) and sparsity of the network is found within a range of $[\frac{2}{N-1}, \frac{4}{N-1}]$. We thus selected p to consider networks filtered to a density of $\frac{3}{N-1}$.

2.2 Network embedding in hyperbolic space

Hyperbolic space is a non-Euclidean space with constant negative curvature. To infer the geometric representations of networks we use a mapping based on the Poincaré disk, which is a two-dimensional model of hyperbolic geometry. The Poincaré disk is a Riemannian manifold where the hyperbolic distance between two points, designated by indices i and j , with polar coordinates (r_i, θ_i) and (r_j, θ_j) , can be computed according to the hyperbolic law of cosines:

$$\cosh d_{hyp}(i, j) = \cosh r_i \times \cosh r_j - \sinh r_i \times \sinh r_j \times \cos(\pi - |\pi - |\theta_i - \theta_j||) \quad (1)$$

In this study, we employ the coalescent embedding method [30] to map brain networks in the Poincaré disk. In a nutshell, for a binary connectivity graph, the method can adjust the weight of edges using a repulsion-attraction rule

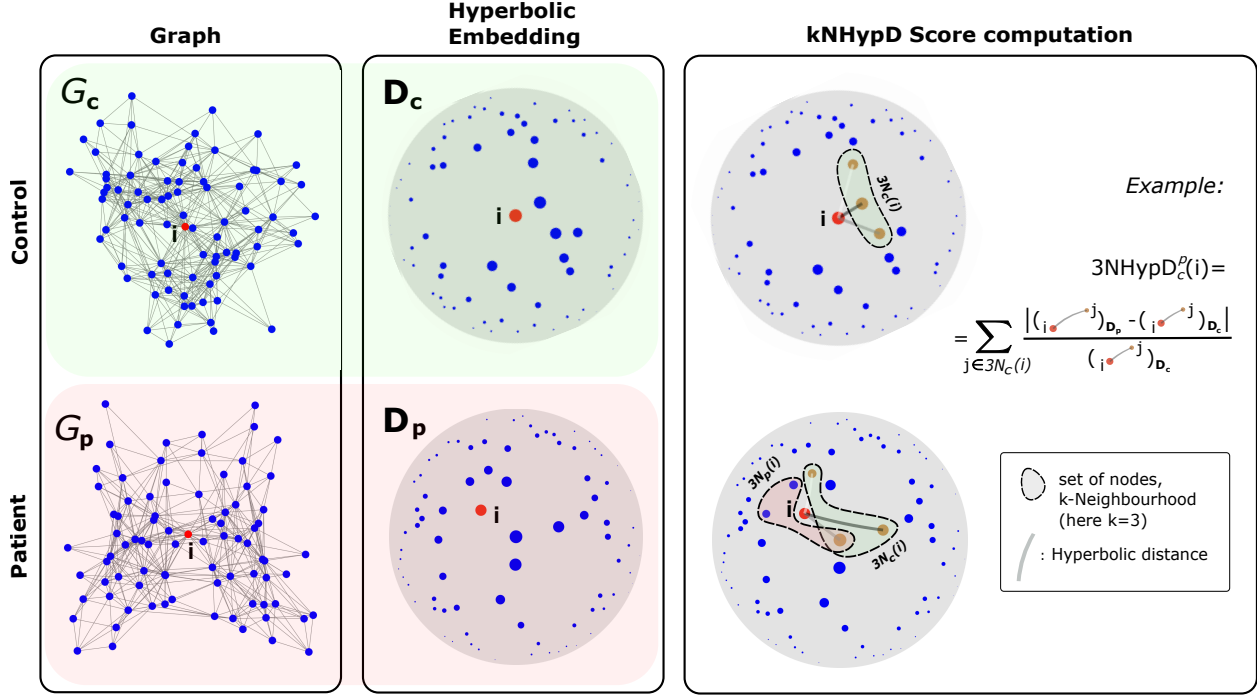


Figure 1: Illustration of the pipeline for the computation of kNHypD score between two brain networks. From left to right: we take the filtered structural brain networks of a patient (graph G_p) and a control (graph G_c); we embed them in a hyperbolic latent space through coalescent embedding [30], obtaining their two-dimensional representations in two Poincaré disks, denoted as \mathbf{D}_p and \mathbf{D}_c ; as an example, we illustrate the computation of the local perturbation of the 3-neighborhood of node i (marked by the red dot in the plots) with the score value $\text{kNHypD}_c^p(i)$, with $k=3$. The set of nodes $3N(i)$ is indicated by the yellow points in the disks.

that prioritizes edges with a more prominent role in information transmission [30]. The resulting weighted connectivity matrix is then projected onto a two-dimensional space with nonlinear dimensional reduction techniques, such as Isomap or Laplacian eigenmaps [38]. In this study, we employed the dimensional reduction technique of Laplacian Eigenmaps as it is computationally efficient and it optimally preserves nodes' local neighborhood information [39]. The angular coordinates of the embedded nodes are adjusted uniformly, while maintaining their angular order. Finally, the radius of each node is assigned as a function of its rank, which is determined by its degree. The radius of each node denotes its centrality, while the angle between them encodes their topological proximity.

In the context of brain networks, the parameters of similarity and centrality are of significant importance in understanding the role of nodes (electrodes, voxels, or regions of interest) in the structure and function of the system. Nodes can be defined as more “similar” if they have a high number of neighbors in common. It can be reasonably assumed that these nodes are likely to belong to the same anatomical region and have similar functional characteristics. It can be observed that brain areas with higher centrality typically play a role of integration within the system, interacting with different anatomical or functional regions, and acting as centers of information sorting. Within the hyperbolic disk, nodes belonging to the same functional or anatomical module will be angularly close, and nodes with the highest centrality will be closer to the center. The hyperbolic distance of Eq. 2.2 combines these two dimensions in a unique proximity concept.

2.3 k -Neighborhood Hyperbolic Distortion score

In this study, we use the geometric perturbation score kNHypD, as presented in [28], to compare brain networks based on their embedded configurations. The k -Neighborhood Hyperbolic Distortion score (kNHypD) is based on the premise that a local perturbation in the connectivity of a node will modify the similarity relations with its neighbors and consequently, their relative distances in the embedding space. To quantify this change at local (nodal) level, we first define the k -neighborhood of node i , denoted as $kN(i)$, as the group of the nearest k neighbors of node i in the embedding space of a graph G , the Poincaré disk \mathbf{D} . In the embedding space of the perturbed graph G' (denoted here as the Poincaré disk \mathbf{D}') node i and its neighbors will have, in general, different coordinates. The k -neighborhood of

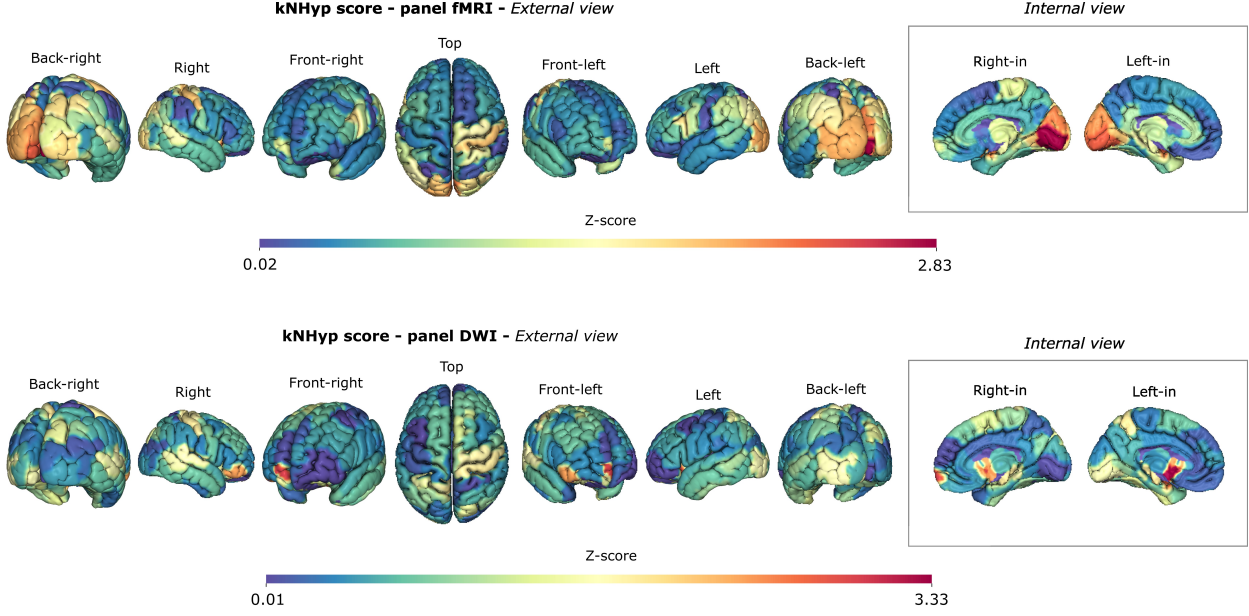


Figure 2: Visualisation of kNHypD score value on a template brain, obtained from the comparison between the two groups of patients and controls, at a parcellation resolution with 128 regions. Top panel is relative to functional brain networks estimated from fMRI, bottom panel is relative to structural brain networks obtained from DWI imaging.

node i in \mathbf{D}' is designated $kN'(i)$, and it defines, in general, a different set of nodes with respect to $kN(i)$. Although the embedding spaces of graphs G and G' have the same metric structure and the same set of embedded nodes, their coordinates are different because the connections they form are different in the original graphs G and G' . For each node i , we compute the distances between i and the points with index $j \in kN(i)$ in disk \mathbf{D} and in disk \mathbf{D}' , respectively. We then compare them by means of the score function [28]:

$$kNHypD(i) = \sum_{j \in kN(i)} \frac{|d_{hyp}(i, j; \mathbf{D}') - d_{hyp}(i, j; \mathbf{D})|}{d_{hyp}(i, j; \mathbf{D})} \quad (2)$$

where the hyperbolic distance $d_{hyp}(i, j; \mathbf{D}')$ denotes the hyperbolic distance 2.2 between the coordinates corresponding to i and j in the embedding disk \mathbf{D}' . The absolute value is introduced to count as a positive contribution both the case of an increase and a decrease of the distance to node i . The score computation is illustrated in Figure 1, with the example of a patient (as a perturbed network) compared with a healthy control.

One of the key advantages of this type of geometric score is its invariance under rotations and reflections of the embedding space. Consequently, in case the embedding algorithm introduces a random component of orientation of the disk, as it is the case of the coalescent embedding [30], there is no need to align the embedded networks prior to their comparison.

The best choice of k in the estimation of kNHypD depends upon the data in question. As with other non-parametric estimators in statistics, a small values of k yields a large variance of the score, while a large number of neighbors increases its bias and the complexity involved in computing a large number of distances [28]. In accordance with the recommendations set forth in [28], we consider a neighborhood size of 10% of the total number of nodes N .

3 Results

3.1 Two-groups kNHypD score

We used this geometric measure to characterize the anomalies of connectivity affecting a group of brain networks of patients diagnosed with Alzheimer's disease, with respect to a group of healthy controls. In this study, we assume that neurodegeneration has caused a perturbation in the organization of the brain network of each patient, compared to

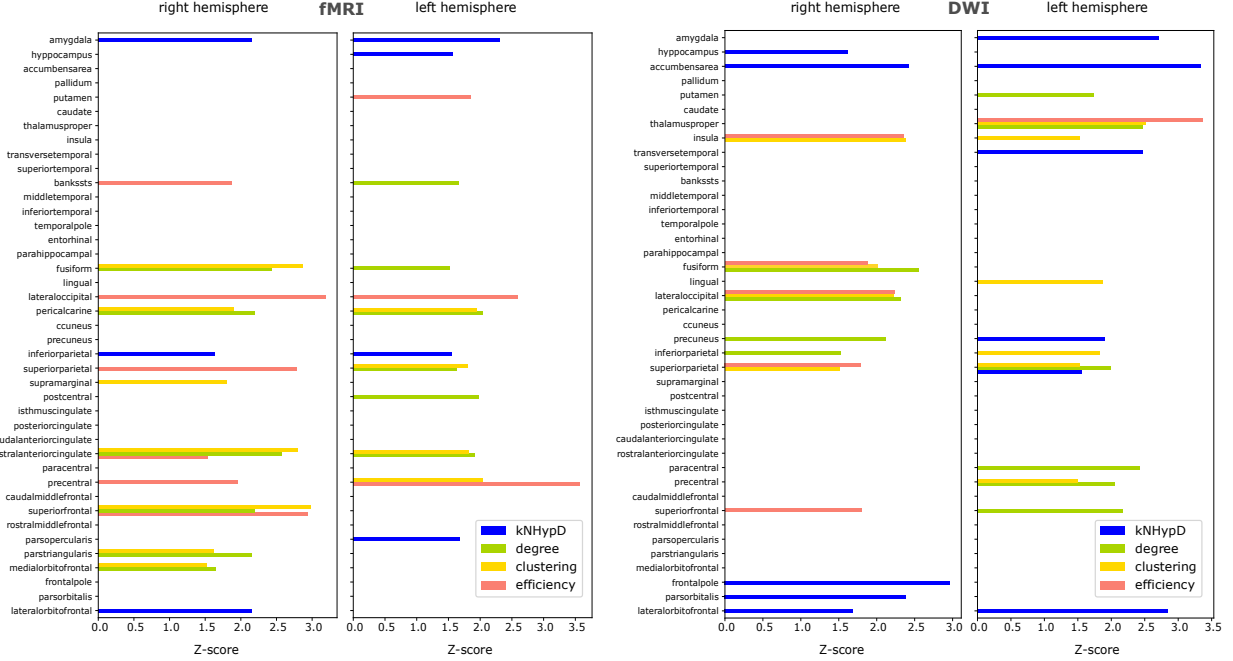


Figure 3: Comparison of areas identified as characteristic areas of connectivity alteration associated with the disease, according to our geometric kNHypD score and to standard topological measures: degree, clustering, efficiency. The magnitude of the bars represents the number of standard deviations from the average over the whole network. Only values above 1.5 are plotted. The networks considered here have $N = 128$ nodes.

the population with healthy characteristics. In this regard, the kNHypD score can be used to localize and quantify the impact of the local perturbation from the geometric distortion of the embedding.

For each brain network G_p with $p \in \mathcal{P}$ (the group of patients), we compute the corresponding embedding in the Poincaré disk \mathbf{D}_p . The same is repeated for the group of controls, \mathcal{C} , obtaining the set of Poincaré disk embeddings $\{\mathbf{D}_c, c \in \mathcal{C}\}$. Then, each patient is compared with each one of the healthy controls, following the scheme illustrated in Figure 1, obtaining the scores $\text{kNHypD}_c^p(i)$ estimating the abnormality of each brain region i of patient p with respect to control c .

$$\text{kNHypD}_c^p(i) = \sum_{j \in kN_c(i)} \frac{|\text{d}_{hyp}(i, j; \mathbf{D}_p) - \text{d}_{hyp}(i, j; \mathbf{D}_c)|}{\text{d}_{hyp}(i, j; \mathbf{D}_c)} \quad (3)$$

The hyperbolic distance $\text{d}_{hyp}(i, j; \mathbf{D}_p)$ is relative to the coordinates that node i and j assume in the hyperbolic embedding of G_p . While $\text{d}_{hyp}(i, j; \mathbf{D}_c)$ is relative to the coordinates they assume in the embedding space of G_c .

We then average over the control group to obtain an absolute set of scores for patient p , which represents the patient's local degree of anomaly with respect to the control population.

$$\text{kNHypD}^p(i) = \frac{1}{|\mathcal{C}|} \sum_{c \in \mathcal{C}} \text{kNHypD}_c^p(i) \quad (4)$$

Finally, we averaged across the group of patients in order to integrate the intersubject variability and infer the areas of connectivity disruption that are most indicative of the disease state.

$$\text{kNHypD}(i) = \frac{1}{|\mathcal{P}|} \sum_{p \in \mathcal{P}} \text{kNHypD}^p(i) \quad (5)$$

It is important to note that each patient's brain network is not being compared with its original, unperturbed configuration prior to the onset of the disease. Instead, it is being compared with a set of control brain networks belonging to different

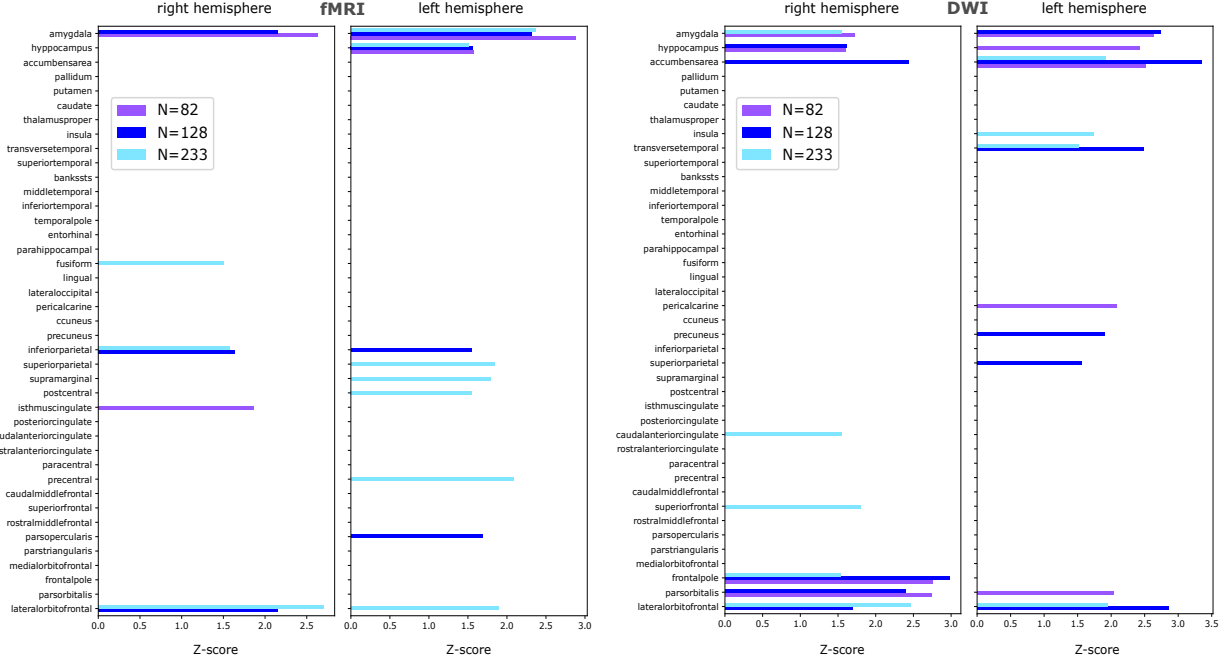


Figure 4: Comparison of anomalous areas identified by the kNHypD score at 3 different parcellation scales of respectively 82, 128 and 233 nodes. The results for the last 2 scales are represented together on the 82 anatomical regions at the lower scale, assigning to the bar the maximum value of deviation over the corresponding subregions. Only bars with magnitude above 1.5 standard deviations are represented.

subjects, which will inevitably exhibit differences in the connections, and thus differences in the geometric embedding configurations, due to intersubject variability. This effect introduce a positive non-zero bias in the value of the kNHypD score estimated at each comparison. To correct for this bias, we identify the regions of the brain exhibiting the highest degree of connectivity perturbation as those exhibiting the highest score relative to the average score calculated over the entire network. The magnitude of the perturbation score will be therefore represented as a Z-score, estimated as the number of standard deviations by which the value deviates from the mean value over the entire network.

The results obtained with the kNHypD geometric score are compared with those obtained from a t-test between the local (node-specific) values of common connectivity measures (degree, clustering, and efficiency). Figure 3 depicts the most abnormal brain areas identified by the different methods, for both fMRI and DWI modalities, and for networks with a parcellation resolution of 128 nodes. For the sake of visualization, only the areas with Z-score values exceeding 1.5 are shown. the presence of positive Z-scores only can be explained considering that the most anomalous values are always larger than the mean.

All the metrics considered identify some regions with significant abnormality in both anatomical (DWI) and functional (fMRI) networks. Those regions belong to the temporal, parietal and frontal lobe, in accordance with the neuropathology of the disease. We suggest that geometric and topological measures convey complementary information about the disruption in the temporal and parietal lobe. We notice, however, that only the geometric score identifies the amygdala, hippocampus and the frontal areas (memory and behavioral-related regions) as affected by the neurodegeneration.

3.2 kNHypD score at multiple scales

We further compared the anomalous regions identified by the geometric kNHypD score at three different resolutions of the parcellation. The results are exposed in Figure 4. We can notice that interestingly, the evidence of connectivity disruption in the amygdala, hippocampus, accumbens area, and the frontal lobe regions is robust across all the different scales analysed. The result relative to DWI networks is characterised by a more important distortion in the right frontal lobe, which can be clearly visualised on the brain map of Figure 2.

Results also show that, in general, different scales contain different informations, which is in agreement with the state of the art on brain network analysis across different parcellation scales [40]. At the lowest resolution of 82 nodes we uniquely find anomalous values in the isthmus of cingulate gyrus for the fMRI, and in the pericalcarine region for the

DWI structural networks. The DWI networks with 128 nodes additionally show anomalies in the precuneus, superior parietal and transverse temporal gyrus. In the fMRI networks instead, main perturbations are found in the inferior frontal and inferior parietal gyri. As for the largest scale ($N = 233$ nodes), we also identify the insula, transverse temporal gyrus, caudal anterior cingulate and superior frontal cortex in the functional networks; while the fusiform, inferior parietal, superior parietal, supramarginal, postcentral and paracentral gyri are identified in the anatomical networks.

Discussion

The application of network science to neurological problems, allowed by the increasing availability of neuroimaging data acquisition and processing techniques, has been proven to be a relevant and non-invasive approach of investigation. In the meanwhile, the field of complex networks has seen the introduction of new models and methods for the analysis of complex systems. Among these, the study of network geometry [41] and the introduction of methods for embedding graphs in a latent low-dimensional hyperbolic space [18] provide novel connectivity information inherent in non-Euclidean embedding spaces. Within these frameworks, the metric structure of the original graph, based on topological distance between nodes (e.g. the shortest paths), is substituted by the metric of the latent space, where distances become geodesics in a manifold (spheres, hyperbolic disks, etc).

In this study, we investigate the advantage of a novel method to study network perturbations, based on geometric embedding of networks in a latent hyperbolic space. We apply it to the task of characterizing connectivity disruption patterns in Alzheimer's disease. We perform the analysis on two-dimensional representations of brain networks in a latent hyperbolic space, obtained through coalescent embedding in the Poincaré disk [30]. We then assign a perturbation score, computed in the Poincaré disk, to each brain region. This method, introduced in [28], is conceived to localize perturbed nodes in complex networks, and applies to our case study assuming the brain network in disease as a perturbation to the healthy ensemble connectivity.

We have shown that the atrophy process associated to the neurodegeneration generates connectivity changes that can be captured in the latent space of brain networks. The proposed score allowed to identify brain regions with a perturbed connectivity in the temporal and parietal lobes, as well as the frontal pole, which have all been found to be involved in the neurodegeneration process. Notably, the detection of abnormalities in memory-related areas (such as the hippocampus and the amygdala) and in the frontal areas, is robust across multiple brain parcellation scales and imaging modalities. Altogether, these results support the hypothesis that AD is a network disease leading to disorganized network configurations at both anatomical and functional level [42, 43].

Notably, the medial temporal regions are crucial for memory and spatial navigation. The hippocampus, along with the amygdala, which is also involved in the memory formation and emotional processing, it is known to be among the first regions to be affected anatomically in Alzheimer's disease. The related clinical symptoms include memory (especially episodic memory) loss, and spatial and temporal disorientation. As expected, the patients included in this study have exhibited clinically significant signs of memory impairment, as reported in Table 1. However, the involvement of the frontal lobes, associated with behavioral and social impairments, did not have a clinical counterpart in our sample. Therefore, we can hypothesize that connectivity changes in these regions precede noticeable clinical changes, making our measure a candidate progression biomarker of the disease. To summarize, our method effectively captures the disruption of brain areas at the network level, not only identifying the areas likely responsible for deficits affecting the patient at the time of the study, but also likely capturing regions that are already affected but clinically silent.

Findings suggest that hyperbolic embeddings allows for an efficient representation of brain networks, encoding multiple non-trivial topological information into the node coordinates, in particular combining the notions of node centrality and similarity. Our score, based on these geometric representations, capture better brain connectivity changes, with respect to standard graph topological metrics. Indeed, we proved the geometric score to be convey complementary information about the changes in the parietal and temporal lobe, but uniquely detecting disruption in the memory related regions and the frontal lobe, which we consider extremely relevant for AD characterization. We notice that the proposed metric can capture various types of connectivity changes. A non-zero score can arise from: *i*) a node that is involved in a disconnection process, which would increase its radius and push it towards the periphery of the hyperbolic disk; or *ii*) a rewiring process, as increasing the degree of a node will bring it closer to the center, modifying its k -neighborhood.

We specify that other non-Euclidean embedding techniques could potentially be combined with the proposed framework to identify local perturbations to the connectivity structure. Alternative hyperbolic mappings (e.g., Mercator [45] HyperMap [46] or Hydra [47] among others) might be worth considering for the representation of brain networks in a lower-dimensional space. Similarly, other dimensionality reduction methods (e.g., Isomap, eigenmaps, ...) could be integrated in the coalescent embedding method to capture the neighborhood information of a network's nodes [38]. The choice of the method can be made depending on the task and demands of the analysis to be performed.

Although theoretical studies support the hypothesis that anatomical brain connections can determine some aspects of dynamics, it is not clear how functional changes could emerge and develop from disconnection patterns initiated by the anatomical atrophy of the brain. By integrating information from structural and functional brain networks in longitudinal studies with healthy subjects progressing into Alzheimer's patients, will be fundamental to provide a more comprehensive insight and understanding of neurodegeneration.

In conclusion, we demonstrate that simple measures in the hyperbolic embedding space are able to capture the typical areas affected by neurodegeneration. Latent hyperbolic space representations of brain networks promise to be the starting point of analyses that could improve our understanding of the brain in health and disease. A longitudinal study could further verify the hypothesis that the functional alteration of the frontal areas here detected precedes the atrophy and onset of clinical signs in patients.

The proposed method is flexible enough to be applied to other clinical cases, namely epilepsy, schizophrenia, Parkinson disease, and many others. Future studies could help to assess the power of hyperbolic latent space representations of networks in localizing subtle yet complex connectivity perturbations, that could be crucial in the characterization and diagnosis of different neurological diseases.

4 Acknowledgments

We have benefited immensely from discussions with many colleagues and friends in the last months but we would like to thank especially Vincent Le Du for his help in the visualization of the results with Visbrain [48, 49]. A.L. acknowledges financial support from the doctoral school EDITE from Sorbonne University, Paris (FR).

References

- [1] C. J. Stam, "Modern network science of neurological disorders," *Nature Reviews Neuroscience*, vol. 15, no. 10, pp. 683–695, 2014.
- [2] C. Manzoni, P. A. Lewis, and R. Ferrari, "Network analysis for complex neurodegenerative diseases," *Current Genetic Medicine Reports*, vol. 8, pp. 17–25, 2020.
- [3] B. M. Tijms, A. M. Wink, W. de Haan, W. M. van der Flier, C. J. Stam, P. Scheltens, and F. Barkhof, "Alzheimer's disease: connecting findings from graph theoretical studies of brain networks," *Neurobiology of aging*, vol. 34, no. 8, pp. 2023–2036, 2013.
- [4] J. Gomez-Ramirez and J. Wu, "Network-based biomarkers in alzheimer's disease: review and future directions," *Frontiers in aging neuroscience*, vol. 6, p. 12, 2014.
- [5] H. Hampel, J. Hardy, K. Blennow, C. Chen, G. Perry, S. H. Kim, V. L. Villemagne, P. Aisen, M. Vendruscolo, T. Iwatsubo *et al.*, "The amyloid- β pathway in alzheimer's disease," *Molecular psychiatry*, vol. 26, no. 10, pp. 5481–5503, 2021.
- [6] C.-Y. Lo, P.-N. Wang, K.-H. Chou, J. Wang, Y. He, and C.-P. Lin, "Diffusion tensor tractography reveals abnormal topological organization in structural cortical networks in alzheimer's disease," *Journal of Neuroscience*, vol. 30, no. 50, pp. 16 876–16 885, 2010.
- [7] P. Joana, v. W. Danielle, S. Erik, S. Tor Olof, V. Giovanni, W. Eric, and H. Oskar, "Abnormal structural brain connectome in individuals with preclinical alzheimer's disease," *Cerebral Cortex*, vol. 28, no. 10, p. 3638–3649, 2018.
- [8] K. Wang, M. Liang, L. Wang, L. Tian, X. Zhang, K. Li, and T. Jiang, "Altered functional connectivity in early Alzheimer's disease: A resting-state fmri study," *Human Brain Mapping*, vol. 28, no. 10, pp. 967–978, 2007.
- [9] A. Badhwar, A. Tam, C. Dansereau, P. Orban, F. Hoffstaedter, and P. Bellec, "Resting-state network dysfunction in alzheimer's disease: a systematic review and meta-analysis," *Alzheimer's & Dementia: Diagnosis, Assessment & Disease Monitoring*, vol. 8, pp. 73–85, 2017.
- [10] Z. Dai, Q. Lin, T. Li, X. Wang, H. Yuan, X. Yu, Y. He, and H. Wang, "Disrupted structural and functional brain networks in alzheimer's disease," *Neurobiology of aging*, vol. 75, pp. 71–82, 2019.
- [11] C. J. Stam, W. De Haan, A. Daffertshofer, B. Jones, I. Manshanden, A.-M. van Cappellen van Walsum, T. Montez, J. Verbunt, J. C. De Munck, B. W. Van Dijk *et al.*, "Graph theoretical analysis of magnetoencephalographic functional connectivity in alzheimer's disease," *Brain*, vol. 132, no. 1, pp. 213–224, 2009.
- [12] W. De Haan, Y. A. Pijnenburg, R. L. Strijers, Y. van der Made, W. M. van der Flier, P. Scheltens, and C. J. Stam, "Functional neural network analysis in frontotemporal dementia and alzheimer's disease using eeg and graph theory," *BMC neuroscience*, vol. 10, pp. 1–12, 2009.

- [13] H. Braak, E. Braak, and J. Bohl, “Staging of alzheimer-related cortical destruction,” *European neurology*, vol. 33, no. 6, pp. 403–408, 1993.
- [14] e. a. Wang, Liang, “Changes in hippocampal connectivity in the early stages of alzheimer’s disease: evidence from resting state fmri.” *Neuroimage*, vol. 31, pp. 496–504, 2009.
- [15] Y. Zhou, J. H. Dougherty Jr, K. F. Hubner, B. Bai, R. L. Cannon, and R. K. Hutson, “Abnormal connectivity in the posterior cingulate and hippocampus in early alzheimer’s disease and mild cognitive impairment,” *Alzheimer’s & Dementia*, vol. 4, no. 4, pp. 265–270, 2008.
- [16] C. R. Jack, D. S. Knopman, W. J. Jagust, L. M. Shaw, P. S. Aisen, M. W. Weiner, R. C. Petersen, and J. Q. Trojanowski, “Hypothetical model of dynamic biomarkers of the alzheimer’s pathological cascade,” *The Lancet Neurology*, vol. 9, no. 1, pp. 119–128, 2010.
- [17] P. Cui, X. Wang, J. Pei, and W. Zhu, “A survey on network embedding,” *IEEE transactions on knowledge and data engineering*, vol. 31, no. 5, pp. 833–852, 2018.
- [18] M. Xu, “Understanding graph embedding methods and their applications,” *SIAM Review*, vol. 63, no. 4, pp. 825–853, 2021.
- [19] M. Xu, Z. Wang, H. Zhang, D. Pantazis, H. Wang, and Q. Li, “A new graph gaussian embedding method for analyzing the effects of cognitive training,” *PLoS computational biology*, vol. 16, no. 9, p. e1008186, 2020.
- [20] P. Goyal and E. Ferrara, “Graph embedding techniques, applications, and performance: A survey,” *Knowledge-Based Systems*, vol. 151, pp. 78–94, 2018.
- [21] G. Rosenthal, F. Váša, A. Griffa, P. Hagmann, E. Amico, J. Goñi, G. Avidan, and O. Sporns, “Mapping higher-order relations between brain structure and function with embedded vector representations of connectomes,” *Nature communications*, vol. 9, no. 1, p. 2178, 2018.
- [22] M. Mach, E. Amico, R. Liegeois, M. G. Preti, A. Griffa, D. Van De Ville, and M. Pedersen, “Connectome embedding in multidimensional graph-invariant spaces,” *bioRxiv*, pp. 2023–04, 2023.
- [23] M. Nickel and D. Kiela, “Poincaré embeddings for learning hierarchical representations,” in *Advances in Neural Information Processing Systems*, vol. 30. Curran Associates, Inc., 2017. [Online]. Available: https://proceedings.neurips.cc/paper_files/paper/2017/file/59dfa2df42d9e3d41f5b02bfc32229dd-Paper.pdf
- [24] W. Whi, S. Ha, H. Kang, and D. S. Lee, “Hyperbolic disc embedding of functional human brain connectomes using resting-state fmri,” *Network Neuroscience*, vol. 6, no. 3, pp. 745–764, 2022.
- [25] I. Chami, Z. Ying, C. Ré, and J. Leskovec, “Hyperbolic graph convolutional neural networks,” in *Advances in Neural Information Processing Systems*, vol. 32. Curran Associates, Inc., 2019. [Online]. Available: https://proceedings.neurips.cc/paper_files/paper/2019/file/0415740eaa4d9dec8da001d3fd805f-Paper.pdf
- [26] D. Krioukov, F. Papadopoulos, M. Kitsak, A. Vahdat, and M. Boguñá, “Hyperbolic geometry of complex networks,” *Physical Review E*, vol. 82, no. 3, p. 036106, Sep. 2010.
- [27] M. Zheng, A. Allard, P. Hagmann, Y. Alemán-Gómez, and M. Á. Serrano, “Geometric renormalization unravels self-similarity of the multiscale human connectome,” *Proceedings of the National Academy of Sciences*, vol. 117, no. 33, pp. 20 244–20 253, 2020.
- [28] A. Longhena, M. Guillemaud, and M. Chavez, “Detecting local perturbations of networks in a latent hyperbolic embedding space,” *Chaos: An Interdisciplinary Journal of Nonlinear Science*, vol. 34, no. 6, 2024.
- [29] C. Baker, I. Suárez-Méndez, G. Smith, E. B. Marsh, M. Funke, J. C. Mosher, F. Maestú, M. Xu, and D. Pantazis, “Hyperbolic graph embedding of meg brain networks to study brain alterations in individuals with subjective cognitive decline,” *bioRxiv*, 2023.
- [30] A. Muscoloni, J. M. Thomas, S. Ciucci, G. Bianconi, and C. V. Cannistraci, “Machine learning meets complex networks via coalescent embedding in the hyperbolic space,” *Nature Communications*, vol. 8, no. 1, p. 1615, Dec. 2017.
- [31] E. Grober and H. Buschke, “Genuine memory deficits in dementia,” *Developmental neuropsychology*, vol. 3, no. 1, pp. 13–36, 1987.
- [32] R. Lemos, M. R. Simões, B. Santiago, and I. Santana, “The free and cued selective reminding test: Validation for mild cognitive impairment and a lzheimer’s disease,” *Journal of Neuropsychology*, vol. 9, no. 2, pp. 242–257, 2015.
- [33] J. Guillou, M. Chavez, F. Battiston, Y. Attal, V. La Corte, M. Thiebaut de Schotten, B. Dubois, D. Schwartz, O. Colliot, and F. De Vico Fallani, “Disrupted core-periphery structure of multimodal brain networks in Alzheimer’s disease,” *Network Neuroscience*, vol. 3, no. 2, pp. 635–652, Jan. 2019.

[34] P. Hagmann, L. Cammoun, X. Gigandet, R. Meuli, C. J. Honey, V. J. Wedeen, and O. Sporns, “Mapping the Structural Core of Human Cerebral Cortex,” *PLoS Biology*, vol. 6, no. 7, p. e159, Jul. 2008.

[35] A. Daducci, S. Gerhard, A. Griffa, A. Lemkaddem, L. Cammoun, X. Gigandet, R. Meuli, P. Hagmann, and J.-P. Thiran, “The connectome mapper: an open-source processing pipeline to map connectomes with mri,” *PloS one*, vol. 7, no. 12, p. e48121, 2012.

[36] S. Achard, R. Salvador, B. Whitcher, J. Suckling, and E. Bullmore, “A resilient, low-frequency, small-world human brain functional network with highly connected association cortical hubs,” *Journal of Neuroscience*, vol. 26, no. 1, pp. 63–72, 2006.

[37] F. De Vico Fallani, V. Latora, and M. Chavez, “A Topological Criterion for Filtering Information in Complex Brain Networks,” *PLOS Computational Biology*, vol. 13, no. 1, p. e1005305, Jan. 2017.

[38] U. Von Luxburg, “A tutorial on spectral clustering,” *Statistics and computing*, vol. 17, pp. 395–416, 2007.

[39] M. Belkin and P. Niyogi, “Laplacian eigenmaps for dimensionality reduction and data representation,” *Neural computation*, vol. 15, no. 6, pp. 1373–1396, 2003.

[40] O. Korhonen, H. Saarimäki, E. Glerean, M. Sams, and J. Saramäki, “Consistency of regions of interest as nodes of fmri functional brain networks,” *Network Neuroscience*, vol. 1, no. 3, pp. 254–274, 2017.

[41] M. Boguñá, I. Bonamassa, M. De Domenico, S. Havlin, D. Krioukov, and M. A. Serrano, “Network geometry,” *Nature Reviews Physics*, vol. 3, no. 2, pp. 114–135, Feb. 2021.

[42] E. J. Sanz-Arigita, M. M. Schoonheim, J. S. Damoiseaux, S. A. Rombouts, E. Maris, F. Barkhof, P. Scheltens, and C. J. Stam, “Loss of ‘small-world’ networks in alzheimer’s disease: graph analysis of fmri resting-state functional connectivity,” *PloS one*, vol. 5, no. 11, p. e13788, 2010.

[43] A. T. Reid and A. C. Evans, “Structural networks in alzheimer’s disease,” *European neuropsychopharmacology*, vol. 23, no. 1, pp. 63–77, 2013.

[44] M. Punzi, C. Sestieri, E. Picerni, A. M. Chiarelli, C. Padulo, A. D. Pizzi, M. G. Tullo, A. Tosoni, A. Granzotto, S. Della Penna, M. Onofri, A. Ferretti, S. Delli Pizzi, and S. Sensi, “Atrophy of hippocampal subfields and amygdala nuclei in subjects with mild cognitive impairment progressing to alzheimer’s disease,” *Heliyon*, vol. 10, no. 6, p. e27429, 2024.

[45] G. García-Pérez, A. Allard, M. Á. Serrano, and M. Boguñá, “Mercator: uncovering faithful hyperbolic embeddings of complex networks,” *New Journal of Physics*, vol. 21, p. 123033, 2019, 118.

[46] F. Papadopoulos, C. Psomas, and D. Krioukov, “Network mapping by replaying hyperbolic growth,” *IEEE/ACM Transactions on Networking*, vol. 23, no. 1, pp. 198–211, 2014.

[47] M. Keller-Ressel and S. Nargang, “Hydra: a method for strain-minimizing hyperbolic embedding of network-and distance-based data,” *Journal of Complex Networks*, vol. 8, no. 1, p. cnaa002, 2020.

[48] E. Combrisson, “Visbrain,” 2018. [Online]. Available: <https://github.com/EtienneCmb/visbrain.git>

[49] V. L. Du, “Visbrain Inria-NERV fork,” 2023. [Online]. Available: <https://github.com/Inria-NERV/visbrain.git>

[50] D. Berron, D. van Westen, R. Ossenkoppele, O. Strandberg, and O. Hansson, “Medial temporal lobe connectivity and its associations with cognition in early alzheimer’s disease,” *Brain*, vol. 143, no. 4, pp. 1233–1248, 2020.

[51] e. a. Wang, Tao, “Multilevel deficiency of white matter connectivity networks in alzheimer’s disease: a diffusion mri study with dti and hardi models.” *Neural plasticity*, 2016.

[52] E. Bullmore and O. Sporns, “Complex brain networks: graph theoretical analysis of structural and functional systems,” *Nature Reviews Neuroscience*, vol. 10, no. 3, pp. 186–198, Mar. 2009.

[53] G. L. Wenk, “Neuropathologic changes in Alzheimer’s disease,” vol. 64. Physicians Postgraduate Press; 1999, 2003, pp. 7–10.

[54] S. E. Rose, F. Chen, J. B. Chalk, F. O. Zelaya, W. E. Strugnell, M. Benson, J. Semple, and D. M. Doddrell, “Loss of connectivity in alzheimer’s disease: an evaluation of white matter tract integrity with colour coded mr diffusion tensor imaging,” *Journal of Neurology, Neurosurgery & Psychiatry*, vol. 69, no. 4, pp. 528–530, 2000.

[55] S. Yan, D. Xu, B. Zhang, H.-J. Zhang, Q. Yang, and S. Lin, “Graph embedding and extensions: A general framework for dimensionality reduction,” *IEEE Transactions on Pattern Analysis and Machine Intelligence*, vol. 29, no. 1, pp. 40–51, 2006.

[56] M. Kitsak, I. Voitalov, and D. Krioukov, “Link prediction with hyperbolic geometry,” *Physical Review Research*, vol. 2, p. 43113, 10 2020.

- [57] F. Papadopoulos, M. Kitsak, M. Á. Serrano, M. Boguñá, and D. Krioukov, “Popularity versus Similarity in Growing Networks,” *Nature*, vol. 489, no. 7417, pp. 537–540, Sep. 2012, arXiv: 1106.0286.
- [58] A. Allard and M. Á. Serrano, “Navigable maps of structural brain networks across species,” *PLoS Computational Biology*, vol. 16, no. 2, p. e1007584, Feb. 2020.
- [59] P. Cui, X. Wang, J. Pei, and W. Zhu, “A Survey on Network Embedding,” *IEEE Transactions on Knowledge and Data Engineering*, vol. 31, no. 5, pp. 833–852, May 2019.
- [60] A. Drzezga, “The Network Degeneration Hypothesis: Spread of Neurodegenerative Patterns Along Neuronal Brain Networks,” *Journal of Nuclear Medicine*, vol. 59, no. 11, pp. 1645–1648, Nov. 2018.
- [61] C. J. Stam, “Modern network science of neurological disorders,” *Nature Reviews Neuroscience*, vol. 15, no. 10, pp. 683–695, Oct. 2014.
- [62] M. Yu, O. Sporns, and A. J. Saykin, “The human connectome in Alzheimer disease — relationship to biomarkers and genetics,” *Nature Reviews Neurology*, vol. 17, no. 9, pp. 545–563, Sep. 2021.
- [63] M. Filippi, S. Basaia, E. Canu, F. Imperiale, G. Magnani, M. Falautano, G. Comi, A. Falini, and F. Agosta, “Changes in functional and structural brain connectome along the Alzheimer’s disease continuum,” *Molecular Psychiatry*, vol. 25, no. 1, pp. 230–239, Jan. 2020.
- [64] H. Zhang, P. D. Rich, A. K. Lee, and T. O. Sharpee, “Hippocampal spatial representations exhibit a hyperbolic geometry that expands with experience,” *Nature Neuroscience*, vol. 26, no. 1, pp. 131–139, Jan. 2023.
- [65] F. Raslau, I. Mark, A. Klein, J. Ulmer, V. Mathews, and L. Mark, “Memory Part 2: The Role of the Medial Temporal Lobe,” *American Journal of Neuroradiology*, vol. 36, no. 5, pp. 846–849, May 2015.
- [66] F. Raslau, A. Klein, J. Ulmer, V. Mathews, and L. Mark, “Memory Part 1: Overview,” *American Journal of Neuroradiology*, vol. 35, no. 11, pp. 2058–2060, Nov. 2014.
- [67] R. de Flores, S. R. Das, L. Xie, L. E. M. Wisse, X. Lyu, P. Shah, P. A. Yushkevich, and D. A. Wolk, “Medial Temporal Lobe Networks in Alzheimer’s Disease: Structural and Molecular Vulnerabilities,” *The Journal of Neuroscience*, vol. 42, no. 10, pp. 2131–2141, Mar. 2022.
- [68] A. L. Smith, D. M. Asta, and C. A. Calder, “The geometry of continuous latent space models for network data,” *Statistical science*, vol. 34, no. 3, p. 428, Aug. 2019.
- [69] P. N. Alves, C. Foulon, V. Karolis, D. Bzdok, D. S. Margulies, E. Volle, and M. Thiebaut de Schotten, “An improved neuroanatomical model of the default-mode network reconciles previous neuroimaging and neuropathological findings,” *Communications Biology*, vol. 2, no. 1, p. 370, Oct. 2019.